

## Supporting Information

### **Cubic MnV<sub>2</sub>O<sub>4</sub> fabricated through a facile sol-gel process as anode material for lithium-ion batteries: morphology and performance evolution**

Ni Wen,<sup>a</sup> Siyuan Chen,<sup>a</sup> Qiuchen Lu,<sup>a</sup> Qinghua Fan,<sup>a</sup> Quan Kuang,<sup>a</sup> Youzhong Dong<sup>a</sup> and Yanming Zhao<sup>\*a,b</sup>

<sup>a</sup>School of Physics, South China University of Technology, Guangzhou, 510640, P. R. China

<sup>b</sup>South China Institute of Collaborative Innovation, Dongguan, 523808, P. R. China

\*Corresponding authors.

E-mail addresses: zhaoym@scut.edu.cn (Y. M. Zhao).

We investigate the structural variations of  $\text{MnV}_2\text{O}_4$  electrode in the initial two cycles over the potential range from 0.01 V to 3 V by employing in-situ XRD tests (Fig. S1). As shown in Fig. S1a, it is clearly seen that all diffraction peaks of  $\text{MnV}_2\text{O}_4$  gradually weakens with the first discharge process being in progress, implying the decomposition of the electrode material. Interestingly, these peaks do not seem to disappear completely, which may be because, on the one hand, the  $\text{MnV}_2\text{O}_4$  is not fully reacted, and on the other hand, the peaks of the newly formed material coincide with some of the peak positions before the decomposition of the  $\text{MnV}_2\text{O}_4$ . In order to further identify  $\text{Li}^+$  ion storage mechanism of the  $\text{MnV}_2\text{O}_4$  electrode in the subsequent cycle, the zoom in the part regions of the in-situ XRD patterns of the  $\text{MnV}_2\text{O}_4$  electrode during the initial two cycles are displayed in Fig. S1b–f. During the first discharge, all newly generated peaks shift subtly toward a lower position. Amazingly, these diffraction peaks recuperate the initial position when fully charging. What's more, these diffraction peaks exhibit the same variation even during the second cycle, proving the occurrence of solid solution behavior, and these peaks should be lithium vanadium oxide solid solution. The periodic evolution phenomenon discloses that subsequent cyclic reactions are reversible after  $\text{MnV}_2\text{O}_4$  is decomposed during the first discharge. Based on the CV and in-situ XRD analysis, the lithium storage mechanism of  $\text{MnV}_2\text{O}_4$  is supposed to be the coexistence of conversion reaction and solid solution behavior. However, contrary to our expectation, no peaks of manganese and its oxides peak can be detected, which may be accredited to the amorphous phase.

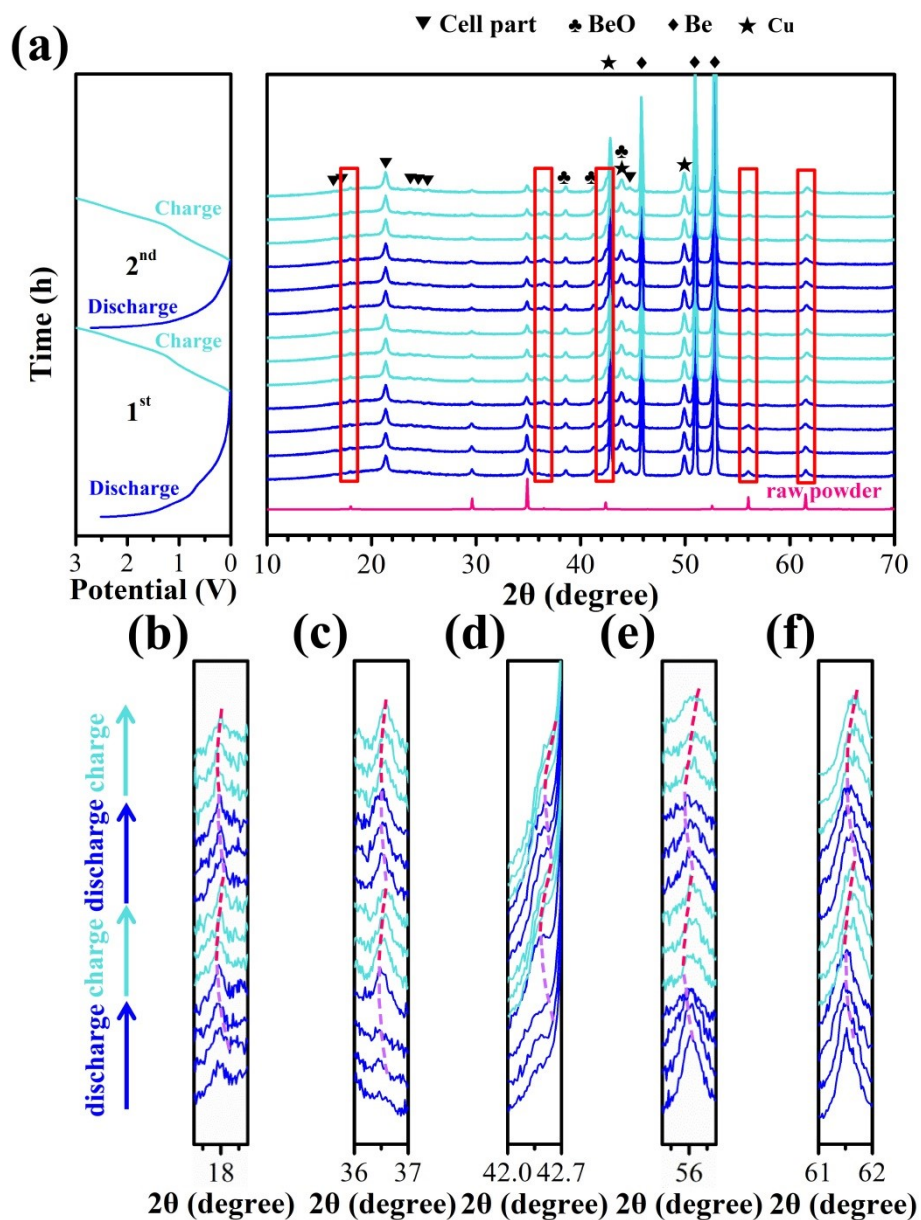


**Fig. S1** (a) Selected in-situ XRD patterns of the  $\text{MnV}_2\text{O}_4$  electrode in the initial two cycles and corresponding discharge/charge curves (left). (b–f) The zoom in the part regions of the in-situ XRD patterns.

**Table S1.** A comparison of electrochemical performances of various spinel-type binary vanadium oxides anode materials.

Anode Materials	Capacity (mAh·g <sup>-1</sup> )	Current Density (mA·g <sup>-1</sup> )	Cycles (n)
Nanophase MnV <sub>2</sub> O <sub>4</sub> particles <sup>1</sup>	550	200	50
MnV <sub>2</sub> O <sub>4</sub> /NC double-layer hollow sandwich nanosheets <sup>2</sup>	717	500	300
Clewlake ZnV <sub>2</sub> O <sub>4</sub> hollow spheres <sup>3</sup>	524	50	50
Hierarchical ZnV <sub>2</sub> O <sub>4</sub> microspheres <sup>4</sup>	638	100	280
Hierarchical mesoporous nanoflowers of Zn <sub>2</sub> VO <sub>4</sub> <sup>5</sup>	528	300	300
Nanoporous CoV <sub>2</sub> O <sub>4</sub> compounds <sup>6</sup>	771	200	100
Spinel Fe <sub>2</sub> VO <sub>4</sub> <sup>7</sup>	225	3 mA·cm <sup>-2</sup>	30
<b>MnV<sub>2</sub>O<sub>4</sub> (This work)</b>	<b>1325</b>	<b>200</b>	<b>500</b>

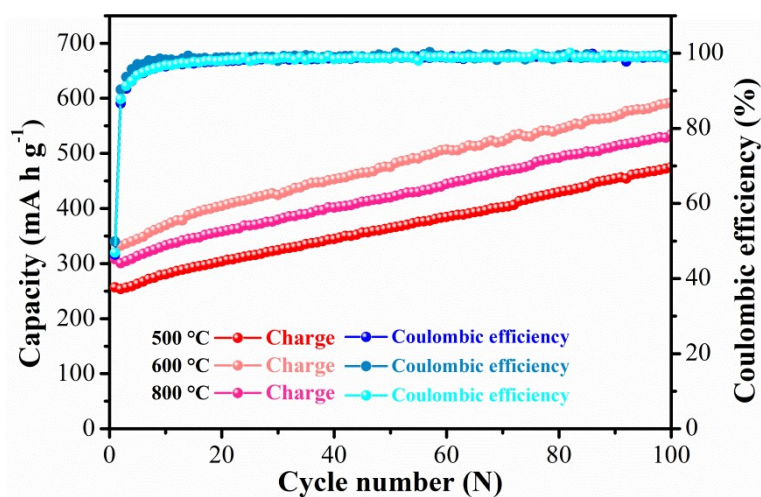


**Fig. S2** Cycling performances and the corresponding Coulombic efficiencies of MnV<sub>2</sub>O<sub>4</sub> prepared at different temperatures at a current density of 200 mA g<sup>-1</sup> within a voltage range of 0.01–3 V versus Li<sup>+</sup>/Li.

The GITT profiles of the MnV<sub>2</sub>O<sub>4</sub> electrodes after 100 cycles, 300 cycles and 500 cycles at a current density of 200 mA g<sup>-1</sup>, respectively, are shown in Fig. S3a. In order to obtain such a continuous curve, the cells need to be discharged/charged at a current density of 200 mA g<sup>-1</sup> with a current pulse duration of 10 min, followed by 100 min interval time. The Li<sup>+</sup> ion diffusion coefficients ( $D_{\text{Li}^+}$ ) of MnV<sub>2</sub>O<sub>4</sub> electrodes can be calculated according to the following equation:<sup>8</sup>

$$D_{\text{Li}^+} = \frac{4}{\pi\tau} \left( \frac{m_B V_M}{M_B A} \right)^2 \left( \frac{\Delta E_s}{\Delta E_\tau} \right)^2 \quad \left( \tau \ll \frac{L^2}{D_{\text{Li}^+}} \right)$$

where  $\tau$  represents the current pulse time,  $m_B$  the mass of the active material,  $M_B$  the molecular

weight,  $V_M$  the molar volume,  $A$  the contact area of electrode-electrolyte,  $\Delta E_s$  the voltage changes caused by the current pulse,  $\Delta E_\tau$  the voltage changes during the constant current pulse, and  $L$  the  $\text{Li}^+$  ion diffusion length equaling to thickness of electrode.

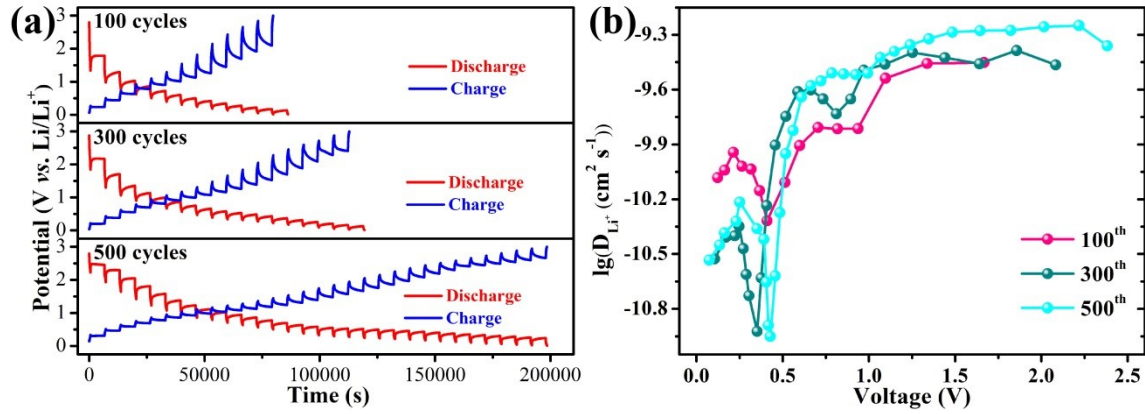


**Fig. S3** (a) GITT profiles of the  $\text{MnV}_2\text{O}_4$  electrodes after 100 cycles, 300 cycles and 500 cycles at a current density of  $200 \text{ mA g}^{-1}$ , respectively. (b) The calculated  $\text{Li}^+$  ion diffusion coefficients.

## References

1. X. Wang, Z. Jia, J. Zhang, X. Ou, B. Zhang, J. Feng, F. Hou and J. Liang, *J. Alloys Compd.*, 2021, **852**, 156999.
2. F. Jing, J. Pei, Y. Zhou, Z. Qin, B. Cong, K. Hua and G. Chen, *J. Colloid Interface Sci.*, 2022, **607**, 538–545.
3. L. Xiao, Y. Zhao, J. Yin and L. Zhang, *Chem. - Eur. J.*, 2009, **15**, 9442–9450.
4. C. Zheng, L. Zeng, M. Wang, H. Zheng and M. Wei, *CrystEngComm*, 2014, **16**, 10309–10313.
5. Z. Tariq, S. U. Rehman, J. Zhang, F. K. Butt, X. Zhang, B. Cheng, S. Zahra and C. Li, *Mater. Sci. Semicond. Process.*, 2021, **123**, 105549.
6. J. Lu, I. Maggay and W. Liu, *Chem. Commun.*, 2018, **54**, 3094–3097.
7. T. Yang, D. Xia, Z. Wang and Y. Chen, *Mater. Lett.*, 2009, **63**, 5–7.
8. Y.-S. Lee and K.-S. Ryu, *Sci. Rep.*, 2017, **7**, 1–13.